Cent. Eur. J. Geosci. • 6(1) • 2014 • 2-16
DOI: 10.2478/s13533-012-0135-6

VERSITA

Central European Journal of **Geosciences**

Relationship between MODIS based Aerosol Optical Depth and PM10 over Croatia

Research Article

Sanja Grgurić[1,2*], Josip Križan[2], Goran Gašparac[2], Oleg Antonić[1,2,3], Zdravko Špirić[1], Rodelise E. Mamouri[4], A. Christodoulou[4], Argyro Nisantzi[4], Athos Agapiou[4], Kyriakos Themistocleous[4], Kurt Fedra[5], Charalambos Panayiotou[6], Diofantos Hadjimitsis[4]

1 *Oikon Ltd.-Institute of Applied Ecology, Trg senjskih uskoka 1-2, Croatia*

2 *Gekom – Geophysical and ecological modeling Ltd., Trg senjskih uskoka 1-2, Croatia*

3 *Josip Juraj Strossmayer University of Osijek, Osijek, Croatia*

4 *Cyprus University of Technology, Lemesos, Cyprus*

5 *Environmental Software and Services, 2352 Gumpoldskirchen, Austria*

6 *Atlantis Consulting Cyprus, Ltd, Cyprus*

Received 22 April 2013; accepted 10 July 2013

Abstract: This study analyzes the relationship between Aerosol Optical Depth (AOD) obtained from Terra and Aqua Moderate Resolution Imaging Spectroradiometer (MODIS) and ground-based PM10 mass concentration distribution over a period of 5 years (2008-2012), and investigates the applicability of satellite AOD data for ground PM10 mapping for the Croatian territory. Many studies have shown that satellite AOD data are correlated to ground-based PM mass concentration. However, the relationship between AOD and PM is not explicit and there are unknowns that cause uncertainties in this relationship.

The relationship between MODIS AOD and ground-based PM10 has been studied on the basis of a large data set where daily averaged PM10 data from the 12 air quality stations across Croatia over the 5 year period are correlated with AODs retrieved from MODIS Terra and Aqua. A database was developed to associate coincident MODIS AOD (independent) and PM10 data (dependent variable). Additional tested independent variables (predictors, estimators) included season, cloud fraction, and meteorological parameters - including temperature, air pressure, relative humidity, wind speed, wind direction, as well as planetary boundary layer height - using meteorological data from WRF (Weather Research and Forecast) model.

It has been found that 1) a univariate linear regression model fails at explaining the data variability well which suggests nonlinearity of the AOD-PM10 relationship, and 2) explanation of data variability can be improved with multivariate linear modeling and a neural network approach, using additional independent variables.

Keywords: MODIS AOD • PM10 • PM10-AOD relationship • aerosol • multivariate linear regression • artificial neural network • Croatia.

*E-mail: sgrguric@oikon.hr

1. Introduction

Particulate matter (PM) is nowadays one of the major air quality issues in Europe [1], as well as in Croatia [2]. Exposure to small particles with diameter size less than 10 μm can lead to respiratory problems and cause premature death [3]. An estimated 5 million years of life are lost per year due to fine particles (PM2.5) alone in the geographic area covering 32 member countries of European Environment Agency (EEA-32) [1]. Therefore, the EU has set limit values for PM10 for daily and annual averages (50 μgm^{-3} and 40 μgm^{-3}, respectively). Daily averages may not be exceeded more than 35 times per year. For PM2.5 an annual average limit of 25 μgm^{-3} has to be reached in 2015 with further reduction to 20 μgm^{-3} to be reached in 2020.

Air quality assessment of PM is usually based on measurement data from established ground monitoring stations. However, these are point measurements and do not provide an adequate spatial coverage to fulfill the needs of mapping regional air quality and human exposure assessments [4]. Another tool for assessing air quality and understanding PM spatial distribution is air quality modeling, which apart from gaps in our knowledge in chemical and physical processes in the atmosphere, suffers mostly from incomplete emission inventory data needed as an input [5]. Although satellite measurements are less precise than ground-based measurements, aerosol optical depth (AOD) retrieved from satellite sensors is considered as a good proxy for ground observed PM mass concentrations and a valuable tool for monitoring aerosol pollution [5–8]. The Moderate Resolution Imaging Spectroradiometer (MODIS) provides distribution of AOD near-globally on a daily basis at spatial resolution of 10 kmx10 km over both ocean and land.

Ground based measurements represent dry mass concentration of PM at the surface, whereas AOD represents the columnar aerosol loading from the surface to the top of the atmosphere [7]. The relationship between these two variables depends on various factors, including aerosol vertical distribution, aerosol type and its chemical composition, as well as its spatial and temporal variability, which are governed by spatio-temporal distribution of emissions and meteorological conditions [8].

During the last decade, various studies have analyzed the relationship between PM and AOD [5, 7–12]. Earlier studies [7, 9, 10] reported a wide range of correlation coefficients (R) for univariate linear regression models (UV) for different areas around the globe. For example, a study of PM2.5-AOD relationship over the entire United States of America (USA), which included 1300 ground monitoring stations, found non-uniform correlations across USA, being strongest in the northeast part of USA ($R > 0.8$) and weakest in the northwestern part of USA ($R < 0.2$), with an average of 0.43 over the entire area [7]. For 26 cities around the globe (in India, Australia, Hong Kong, United States of America and Switzerland), R ranged from 0.11 to 0.85 [10]. Although AOD and PM correlate well for some regions and in specific situations with stable meteorological conditions and fixed pollution sources [8], most of these studies have concluded that AOD alone do not explain surface PM concentrations well, since other factors affect the PM-AOD relationship (such as the vertical distribution of aerosols, aerosol type and chemical composition, its temporal variability, and meteorological parameters).

In situations with aerosols transported aloft - which ground monitors may not capture - columnar AOD and surface PM mass concentration may not correlate well. Additionally, satellites can measure almost the same columnar AOD during two different conditions: one with low planetary boundary layer height (PBLH) when surface PM concentrations can be high (if aerosol is confined within planetary boundary layer); and second with high PBLH when surface concentrations are low (when diluted in vertical column) [12]. Ground and space borne lidars, such as Cloud Aerosol and Infrared Pathfinder Satellite Observation (CALIPSO) provide information on vertical distribution of aerosols that can help assess whether the aerosol is confined to the surface planetary boundary layer (PBL) or aloft [13]. Moreover, lidar apportionment of the fraction of aerosol optical depth that is within the PBL can be scaled to give better agreement with surface PM than does the total column amount [13].

However, there are limitations with these data. CALIPSO provides observations in a very narrow swath and global coverage is reached only after several weeks. On the other side, ground-based lidars are spatially very sparse and do not operate continuously. Although these data cannot be used for spatial mapping of daily averaged PM concentration, it can be useful for interpretation and improvement of the PM-AOD relationship by finding the most significant upper-level transport events. As some studies (using limited observations of vertical distribution of aerosols from lidars) have demonstrated that aerosols are well mixed and mostly confined within the PBL, a PBLH can be used as a surrogate to estimate the height of the aerosol layer [12]. Other meteorological parameters influencing PM-AOD relationship are humidity (due to hygroscopic growth of particles and production of secondary particles), temperature (T) (due to effect on photochemical reactions in which PM particles are produced), wind speed (WS) (affecting horizontal and vertical dispersion), and temperature vertical gradients (affecting vertical mixing). A detailed discussion on meteorological parameters

affecting PM concentration is given in Gupta and Christopher, 2009 [12].

Inclusion of meteorological parameters, such as PBLH, WS and relative humidity (RH) into PM-AOD relationship, improved estimation of PM2.5/PM10 concentrations using multivariate linear (MV) and non-linear regression models compared to UV model [5, 10, 12, 14]. For example, average R over the entire Europe (not including Croatia) improved from 0.3 to 0.5 (0.6) for PM10 (PM2.5) with inclusion of PBLH and RH into the PM-AOD relationship, where R varied in respect to location and season [5]. In recent studies, an artificial neural network (ANN) was applied to estimate PM2.5, taking into account T, RH, WS and PBLH [15, 16]. The estimates of PM2.5 with ANN for 85 monitoring stations across the USA improved (R = 0.83) compared to UV (R = 0.67) and MV (R = 0.77) models, indicating that a neural network approach is better suited for deriving PM-AOD relationship [15]. The study with application of ANN in China [16] obtained R that varied both with location and season (the highest R being 0.74). Those studies concluded that PBLH is one of the dominant factors determining the performance of ANN.

The objective of this study was to explore the possibility of spatial mapping of surface PM10 concentrations with spatially generalized model for Croatia using satellite data in order to obtain estimates for areas where measurements do not exist, that currently covers almost half of 20 counties in Croatia. The PM10-AOD relationship has been assessed using four different empirical models in order to find the model with best estimates: univariate linear regression model (UV); multivariate linear regression model with first order effects (MV1), multivariate linear regression model with first and second order effects (MV2) and artificial neural network (ANN) model, using meteorological parameters as independent predictors.

2. Data and methodology

2.1. Data

Assessment of the PM10-AOD relationship has been performed using three different datasets over a period of 5 years (2008-2012): 1) hourly surface PM10 mass concentrations measured at 12 ground-based stations (see Figures 1 and 2); 2) Terra and Aqua MODIS AOD at 0.55 μm and Cloud Fraction (CF); and 3) meteorological parameters from WRF meteorological model over above mentioned 12 stations in Croatia.

2.1.1. Surface PM10 mass concentration

Surface PM10 mass concentration data were obtained from Air Quality Database of Croatian Environment Agency Information System. The Croatian air quality monitoring network consists of national and several local networks of ground measurement stations and it is still under development. Currently, PM10 is monitored by 28 ground stations. Measurement methods are not unified across stations, including mostly beta-absorption measurement method and referent gravimetric method. This study uses hourly PM10 mass concentration data from 12 ground monitoring stations, which met criteria of 70% data capture through the period of 5 years. These stations are equipped with automatic analyzers that utilize beta-absorption method. The data were taken as measured, without application of correction factors that should result from a test of equivalency with referent gravimetric method, due to lack of such tests for all stations. Among the 12 chosen stations (Figure 1 and 2), 11 are urban, dominated by emission sources from industry and traffic, and only 1 station is rural, dominated by industrial emission sources (rural background stations are still under development). Five of these stations are located in the coastal area, and seven in the continental part of Croatia.

2.1.2. Satellite aerosol data

The MODIS instruments onboard the Terra (crossing Europe ~10:30 local time) and Aqua (crossing Europe ~13:30 local time) satellites provide routine retrievals of cloud and aerosol properties in seven different spectral bands over the ocean and in three bands over land [18]. This study uses AOD and CF data from the new MODIS algorithm (collection C051, based on the operational algorithm V5.2) that incorporates improved estimation of surface reflectance (for land) and applies stringent criteria to select appropriate pixels in the retrieval process, compared to collection C004 (V5.1) [17].

The AOD algorithms for land and ocean are independent and different, due to different radiative properties of land and water. The retrieval of AOD is based on analyzing 20 × 20 pixels at 500 m resolution and reported at 10 × 10 km^2 resolution. The ocean algorithm is applied only if all 400 pixels are identified as ocean pixels. If any land is contained within the 10 km × 10 km cell, the land algorithm is applied [18]. The retrieval is considered more accurate over ocean than over land, validated against ground-based AErosol RObotic NETwork (AERONET), where one standard deviation of AOD fell within the expected uncertainty level of ±0.03±0.05 AOD over ocean and of ±0.05±0.15 AOD over land [17, 18]. This is because the reflection by water is homogenous, relatively low and well known [18]. The operational product Optical Depth Land and Ocean (AOD at 0.55 μm band for ocean (best) and land (corrected) with best quality data (Quality Flag = 3) has been used in our study.

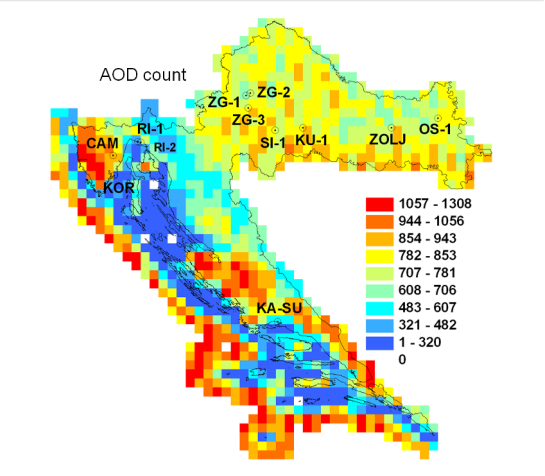

Figure 1. Number of days with available AOD data in the period 2008-2012. Labels represent locations of ground-based PM10 measurement stations.

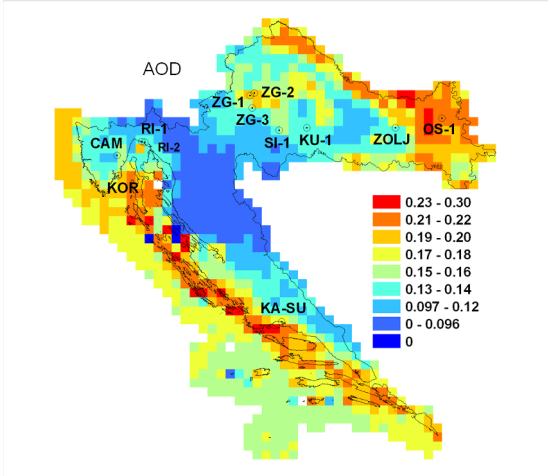

Figure 2. Five-year (2008-2012) average of daily MODIS AOD values. Labels represent locations of ground-based PM10 measurement stations.

The sources of uncertainties in MODIS AOD include instrument calibration errors, cloud-masking errors, incorrect assumptions on surface reflectance, and aerosol model (fine or coarse mode) selection [18].

The smallest number of AOD values in the 5 year period was retrieved for marine coastal area, with numerous islands (approx. 1000) (Figure 1). Within that area, it is likely that application of the land algorithm to fragments of sea resulted in high AOD values [19] (Figure 2), as there are no known sources or reasons for increased aerosol pollution at that area. However, there were no available ground-based AOD measurements for that area to check those AOD values. Spatial distribution of averaged AOD values for the period of 5 years for the inland part of Croatia shows increased values in the most populated, central part of Croatia and in the eastern, agricultural area (Figure 2).

2.1.3. Meteorological variables from WRF model

This study uses hourly analysis data of planetary boundary layer height (PBLH), air temperature at 2 m height (T), surface relative humidity (RH), wind speed (WS), wind direction (WD) and surface pressure (P). These meteorological variables were obtained with Weather Research and Forecasting (WRF) mesoscale numerical model V.3.3.1 [20]. The configuration of WRF model consists of parent domain with horizontal resolution of 18 km × 18 km, encompassing countries surrounding Croatia, and one nested domain with horizontal resolution of 6 km × 6 km covering the entire of Croatia. Initial and boundary conditions stemmed from NCEP FNL (National Centers for Environmental Prediction Final Analyses) that is provided globally on 1° × 1° grid every 6 h (FNL ds083.2). FNL analysis is a quality-assured/quality-controlled product from Global Data Assimilation System (GDAS) which continuously produce multiple analyses on collected observational data from Global Telecommunications System (GTS) and various other sources (e.g., synoptic stations, radiosondes, aircrafts, satellites) provided by different countries and organizations and assimilated by a modern analysis/forecast system to obtain a physically and thermodynamically consistent global reanalysis of atmospheric fields. The output frequency of WRF model was set to 1 hour. The integration time step was set to 108 seconds. Vertically, the model had 35 unequally spaced sigma levels that are more densely distributed near the ground. For parameterization of the boundary layer we used the YSU (YonSei University) scheme with UNLSM model (Unified Noah Land-Surface model) for surface [21, 22] and WSM (WRF Single-Monent) 6-class Microphysics scheme [23]. For radiation parameterization, a Rapid Radiative Transfer Model (RRTM) [24] scheme was used for longwave, and Goddard short wave for shortwave radiation [25]. For cumulus parameterisation a Kain-Fritsch (new Eta) scheme was used [26].

2.1.4. Data integration and averaging schemes

Ground-based measurements are point values, whereas MODIS AOD represents average values in 10 km × 10 km pixels, and meteorological fields from WRF represent point values in 6 km × 6 km grid. In order to integrate those values into the process of estimating surface PM10 mass concentrations, 5 years (2008-2012) of coincident data from three different sources were collocated at the same

temporal and spatial scales. As for the temporal scale, hourly ground-based PM10 mass concentrations were averaged over the period between 10:00 and 14:00 local time, that corresponds with the period of Terra and Aqua satellite passes. The same temporal averaging scheme was applied to hourly meteorological fields from WRF. As our PM10 measurement stations are mainly urban and located in areas with complex topography, as an appropriate spatial averaging scheme we have chosen averaging of MODIS Terra and Aqua AOD data over pixels whose centers fall into a 10 km radius circle centered over surface measurement stations, for each day. Meteorological parameters from WRF model were interpolated from a 6 km × 6 km grid to locations of ground-based PM10 measurement stations using bilinear interpolation. The matched data set contains spatio-temporally collocated "daylight" daily average of satellite-derived AOD and CF, surface PM10 measured mass concentration and WRF derived meteorological parameters. The final data set contains 7114 collocated samples, used for development, testing and validation of statistical models.

2.2. Overview of the spatial and temporal variability of independent variables

The mean (±standard deviation) AOD value of the whole data set is 0.16±0.13 and the mean (±standard deviation) PM10 mass concentration is 26.65±17.18 (see Table 1). Both AOD and PM10 show an overall decreasing trend of aerosol pollution in Croatia in the period from 2008 to 2012 (Figure 3). The highest decrease of PM10 annual means was from 36.10 μgm^{-3} in 2008 to 23.45 μgm^{-3} in 2010. From 2010 to 2012 it increased mildly to 24.67 μgm^{-3} in 2011 and then decreased again to 22.85 μgm^{-3} in 2012. The mean AOD decreased from 0.18 in 2008 to 0.14 in 2012 with an exception of slight increase of 0.003 in 2009. All the variables show significant seasonal variability. AOD values are the highest in spring (0.20±0.14) and the lowest in winter (0.11±0.09). On the other hand, PM10 values are the highest in winter (30.09±24.18 μgm^{-3}) and autumn (29.27±19.96 μgm^{-3}) and the lowest in spring (25.28±13.30 μgm^{-3}) and summer (25.09±15.14 μgm^{-3}). Such seasonal PM10 variability is present only at continental stations, probably due to combination of emissions from household heating and unfavorable meteorological conditions (e.g., temperature inversions) that prevent dispersion of pollution during colder parts of the year. A planetary boundary layer is the highest in summer (1.48±0.63 km), followed by spring (1.43±0.64 km) and the lowest in winter with mean values of 0.71±0.41 km. It is on average higher at continental stations (1.51±0.58 km)

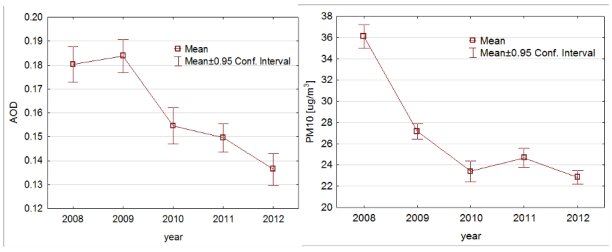

Figure 3. Five-year (2008-2012) trend in annual mean of AOD (left) and PM10 mass concentration (right).

than at coastal stations (0.89±0.51 km). The coastal stations have on average lower AOD (0.14±0.12) and PM10 (20.40±13.83 μgm^{-3}) than continental stations (AOD 0.17±0.14; PM10 30.69±17.76 μgm^{-3}). Relative humidity mean values vary between 46% (summer) and 53% (winter). Wind speed is the highest in the winter (4.14±3.37 m/s) and the lowest in the summer (2.46±1.50 m/s) and it is on average higher at coastal stations (3.6±2.92 m/s) than at continental stations (2.4±1.29 m/s).

2.3. Development of empirical models (univariate model, multivariate linear models, ANN)

Previous studies have demonstrated that the variability of surface PM mass concentration can be better explained with multivariate regression models (both linear and nonlinear) as well as with artificial neural networks (using meteorological parameters as additional independent predictors) than with univariate linear regression model (with AOD as predictor) [14–16]. Additionally, the neural network approach has been widely used in atmospheric and air quality modeling studies [27, 28] and demonstrated to be effective for air pollution estimation and prediction.

In this study we analyzed and compared the PM10-AOD relationship using four models: 1) univariate linear regression model (UV); 2) multivariate linear regression model with first-order effects (MV1); 3) multivariate linear regression model with first and second-order effects of the independent variables (MV2) and 4) artificial neural network (ANN). The MV1 and MV2 models were built with "best-subset" building method, using Mallows' CP [29] as the criterion for choosing the best subset of predictor effects. This measure of the quality of fit for a model tends to be less dependent (than the R-square) on the number of effects in the model, and hence, it tends to find the best subset that includes only the important predictors of the respective dependent variable.

The independent continuous variable used as predictor of surface PM10 mass concentrations for UV model was

AOD. For multivariate and ANN models tested continuous variables were AOD, PBLH, RH, WS and WD, T, P and CF. All the variables have been taken as measured or obtained by meteorological model, with exception of wind direction. Due to the fact that this variable is circular (0°= 360°), it is represented by eastern (U_n) and western (V_n) wind components, which were previously normalized with WS to interval [-1 1], since the WS is already included as independent variable. PM10, AOD and the most meteorological parameters show significant seasonal variability, as presented in section 2.3. Previous studies found seasonal differences in the PM-AOD relationship, where larger errors were associated with PM estimation for winter, when meteorological conditions - such as low temperature and shallow boundary layer - may lead to poor PM estimation, e.g. [12]. During the summer, the planetary boundary layer is deeper and well mixed and in such a situation columnar measurements are better correlated with surface level pollution [13]. Hence, it is expected that adding a "season" as a categorical predictor will improve models' performance. In order to test this assumption, two variants of each of four models were developed: Variant 1, that assumes models without categorical predictors, and Variant 2 that includes "season" as a categorical predictor. In the first three type of models (UV, MV1, MV2), the categorical predictor "season" was coded using the sigma-restricted parameterization [30]. Descriptive parametric and non-parametric statistics of independent continuous variables is given in Table 1. The quantitative description of linear regression models (equations and regression parameters) is given in Appendix A.

As a fourth model, a multi-layer perceptron (MLP) feed forward type of neural network was chosen [31, 32]. In general, artificial neural networks (ANN) represent a numerical method that simulates the biological brain used for learning and recognizing patterns in data sets, as they predict desired output data based on the provided input data. They can be used in many cases for regression and classification tasks. The most commonly used type of neural networks is a feed forward multilayer perceptron (MLP). An artificial neural network commonly consists of three or more layers of neurons: the input layer, one or more hidden layers, and an output layer. Output of every neuron is connected with all neurons in the next layer (Figure 4). Every connection has its weight and every neuron has a bias and activation function. Weights and biases are unknown parameters that need to be obtained from training data. Output of the *j-th* neuron is calculated as:

$$z_j = g\left(\sum_i a_i w_{ij} + b_j\right), \tag{1}$$

where a_i is the output of the *i*-th neuron in previous layer,w_{ij} is a weight of connection from that neuron to *j-th* neuron in the current layer, b_j is the bias of *j-th* neuron and g is an activation function of *j-th* neuron. We used one of the most common, a logistic sigmoid activation function, given by

$$g(x) = \frac{1}{1 + e^{-x}}. \tag{2}$$

The complexity of ANN depends on a number of weights and biases which depends on number and size of hidden layers. Finding these parameters from training data is referenced as training of neural network. In this study, the *ffnet* module for Python [33] was used for development of ANNs. It is a quick and easy-to-use feed-forward neural network training solution package that uses feed-forward architecture and a sigmoid activation function. In the Python package, several methods for training ANNs have been implemented. We have chosen the *rprop* algorithm, originally designed by Riedmiller and Braun [34], because of its speed and simplicity. It is a widely used algorithm especially for multilayer feed-forward networks designed to overcome inherent disadvantages of earlier gradient-descent algorithm. If the number of parameters is too small, ANN will have poor fit on training data. If the number of parameters is too large, ANN will have good fit on training data but will fail to generalize to new data ("overfitting"). One way to overcome this problem is a method of early stopping [31] where training is stopped when error (measured with respect to independent data set not used for training) started to increase. That data set is generally called the validation data set. To get an optimal ANN architecture (number of hidden layers and neurons) we have trained many instances of ANNs of specific architecture using early stopping method (1-2 hidden layers with 10-30 hidden neurons per layer). To construct each of these ANNs, the dataset was randomly split into training (60%), validation (20%) and test (20%) datasets. Because there are many ANNs trained, there is a chance that network with best performance on validation data set might not be the one with the best performance on new test data. Therefore we need test data set which is used only once on every trained network and the network with the best performance on test data set is chosen as the best.

This procedure is used for both Variant 1 and Variant 2 ANN models. Performance of trained ANNs is measured by using the Root Mean Square Error (RMSE) statistic, given by

$$RMSE = \sqrt{\frac{1}{n}\sum_{i=1}^{n}(p_i - o_i)^2}, \tag{3}$$

Table 1. Descriptive (parametric and none parametric) statistics for independent variables in modeling dataset (7114 samples): Mean, Standard Deviation (Std), Minimum (Min), 10^{th} percentile (p10), Median (Med), Median Absolute Deviation (Mad), 90^{th} percentile (p90) and Maximum (Max).

Statistics	PM10 (μgm^{-3})	AOD	T (°C)	PBLH (km)	P (hPa)	RH (%)	WS (m/s)	Un (m/s)	Vn (m/s)	CF
Mean	26.65	0.16	21.27	1.27	1017.94	48.69	2.87	−0.02	0.15	0.06
Std	17.18	0.13	7.65	0.64	5.91	11.87	2.15	0.68	0.64	0.12
Min	0.15	0.00	−5.91	0.01*	988.01	19.71	0.23	−1.00	−1.00	0.00
p10	9.28	0.02	9.90	0.43	1011.43	34.50	1.12	−0.93	−0.84	0.00
Med	23.40	0.13	22.95	1.27	1017.52	47.34	2.27	0.03	0.29	0.00
Mad	12.44	0.10	6.25	0.53	4.46	9.41	1.43	0.62	0.57	0.09
p90	46.78	0.33	29.85	2.11	1025.44	64.95	5.19	0.85	0.90	0.23
Max	190.95	1.96	36.57	3.26	1044.84	100.00	19.57	1.00	1.00	0.80

*This unrealistically low PBLH value (0.01) is a probable consequence of WRF model error at one single coastal station (KA-SU).

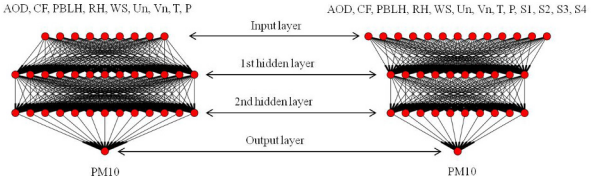

Figure 4. The optimal neural network architecture for surface PM10 concentration estimation. Left: ANN in Variant 1 without seasons as independent variables. Right: ANN in Variant 2 with seasons coded as S1-winter, S2-spring, S3–summer and S4-autumn. Each red circle represents one neuron in ANN. Output of each neuron (except neurons in the input layer) is calculated according to Eq. 1.

where n represents the number of samples, p_i the estimated PM10 concentration, and o_i the observed PM10 concentration. The optimal neural network architecture for Variant 1 consists of 9 neurons in input layer (predictors), 2 hidden layers with 13 neurons in each of them, and one output layer node (with PM10 surface mass concentration as output), whereas in Variant 2, ANN has 13 neurons in input layer (the same variables as in Variant 2 plus seasons), 2 hidden layers with 10 neurons in each (Figure 4). The number of ANN model parameters is 326 in Variant 1, and 261 in Variant 2.

3. Results and discussion

3.1. Overall model performance

The overall performance of four different models is summarized in Table 2 in terms of RMSE defined by Eq. 3 and linear correlation coefficient (R) given by

$$R = \frac{\sum_i (o_i - \overline{o})(p_i - \overline{p})}{\sqrt{\sum_i (o_i - \overline{o})^2 \sum_i (p_i - \overline{p})^2}}. \quad (4)$$

The overall performance is the poorest for UV model and increases as the model complexity increases (from UV to ANN), for both variants (with and without season as a categorical predictor), as was expected. R is significantly higher (R difference test, $p < 0.01$) for all linear models (UV, MV1, MV2) in Variant 2 than in Variant 1. In the case of ANN, adding season as a categorical variable doesn't significantly change the correlation coefficient ($p > 0.01$). It appears that the neural network recognizes seasonal patterns from meteorological parameters, without categorical addition of seasonality. As our goal was to find the most suitable model for PM10 mapping and there was no special reason not to include season as an independent variable, only models in Variant 2 are discussed further on. Overall improvement of more complex models compared to UV model, in terms of the percentage increase of R is 53.1% for MV1, 65.6% for MV2 and 90.6% for ANN. The RMSE decreases the most for ANN (21.4%) but less so for MV1 (7.9%) and MV2 (10.1%). The correlation coefficients for UV and MV1 are similar to other findings for locations in Europe [5, 12].

The procedure of finding the best model subsets in case of MV1 and MV2 (using Mallows' CP criterion) revealed significant contribution (for which $p < 0.01$) of the following variables, listed in order of significance of contribution for MV1: AOD, WS, Vn, RH, PBLH, Un, T CF, P; and for MV2: AOD, WS, PBLH, $PBLH^2$, T^2, RH^2, AOD^2, Vn, T.

Sensitivity analysis for ANN which is capable of recognizing and learning complex patterns in data, showed sensitivity for all input variables (using F-test for comparison

Table 2. Statistics (R, RMSE) of four model types (UV, MV1, MV2, ANN) performance for two variants, the first without categorical independent variables, and the second with season as a categorical independent variable. RMSE is given in μgm^{-3}.

Model type->	UV		MV1		MV2		ANN	
Performance measure->	R	RMSE	R	RMSE	R	RMSE	R	RMSE
Variant1-without categorical variables			N=7114				N=1453 (test data set)	
Overall performance	0.28	16.49	0.45	15.36	0.49	15.02	0.60	12.99
Variant 2 - with season as categorical variable			N=7114				N=1453 (test data set)	
Overall performance	0.32	16.26	0.49	14.98	0.53	14.62	0.61	12.78

of variances, $p < 0.01$), meaning that exclusion of one the parameters would result in a significant difference in the variance of error.

3.2. Model performance by seasons

Performance of all models varies by seasons (Table 3). Seasons are defined as winter (December - February), spring (March-May), summer (June-August), and autumn (September-November). The simplest model (UV) has the poorest performance in winter (R=0.26, RMSE=23.53 μgm^{-3}); this could be associated with lower PBLHs (compared to other seasons) that do not allow mixing in longer air column, and so could affect the PM10-AOD relationship [12]. Performance in winter improves with inclusion of meteorological variables, where ANN shows the highest rate of improvement (161% for R, and 23% for RMSE). In the case of winter, MV1 model performs slightly better than the more complex MV2 model. For all other seasons, model performance increases with increase in model complexity, where the ANN has the highest rate of improvement for all seasons. The linear correlation coefficient for MV1, MV2 and ANN models is the highest for autumn (0.53, 0.60 and 0.69, respectively) and the lowest for spring (0.43, 0.45 and 0.49, respectively).

The seasonal variability of R reflects the complexity of the relationship between dependent (PM10) and independent variables (AOD, CF, meteorological parameters) and has to be the subject of future research. Possible causes for this variability are: 1) seasonal variations in aerosol vertical profile that affect AOD-PM10 relationship, 2) seasonally variable transport of aerosol in upper layers, 3) seasonal variations of uncertainties in AOD related to temporal heterogeneity of aerosol type and composition (not included in assumed model used in MODIS aerosol retrieval algorithm) and 4) seasonal variations in accuracy of meteorological parameters obtained by WRF model (caused by complex topography and climatic characteristics of the study area).

3.3. Model performance by stations

The performance of all models varies with geographic locations (Figure 5). A comparison of model performance by station shows that inclusion of meteorological variables (within MV1, MV2 and ANN models) leads to improvement of PM10 estimates at all stations (Figure 5), compared to simple UV model. Average improvement rate of R over all stations is 50.2% for MV1, 61.3% for MV2 and the highest for ANN (74.6%). However, ANN doesn't perform better equally at all stations compared to MV1 and MV2 models, where R ranges from 0.39 to 0.75. At three coastal stations (KA-SU, KOR, RI-1) performance of ANN is similar to MV2 where both ANN and MV2 perform better than MV1. At one coastal station (RI-2) performance of the ANN model shows no improvement over simpler MV1 and MV2 models (Figure 3). Similar findings for the poorer performance of ANN estimates of PM2.5 for coastal stations have been already reported by Gupta and Christopher [14]. This could be related to higher uncertainties associated with satellite retrievals that contain mixed land and sea surface reflectance, which may lead to high AOD values [18], as well as to higher uncertainties of modeled meteorological parameters at the land-sea boundaries, due to the complex topography at the coastal area.

Additionally, it has to be emphasized that continental stations, which have higher mean and variability of PM10 values than coastal stations, are better represented by neural network due to larger dataset (N=4425, in comparison to N=2689 for coastal stations). The performance of ANN improved the most for ZG-1, ZG-3 and OS-2 stations, all being continental stations. We will further discuss performance of the ANN model as it shows the best overall performance.

3.4. ANN residuals

The differences between observed and estimated PM10 concentrations (residuals) for ANN by seasons and stations are given in Figure 6. Negative residuals point to

Table 3. Comparison of performance of different models in Variant 2 (with "season" as categorical variable) by seasons in terms of linear correlation coefficient (R) and Root Mean Square Error (RMSE). RMSE is given in μgm^{-3}. The numbers in parenthesis represent percentage improvement over univariate (UV) model.

Model type->		UV		MV1		MV2		ANN	
	N	R	RMSE	R	RMSE	R	RMSE	R	RMSE
Winter	665	0.26	23.53	0.52 (105)	20.86 (11)	0.49 (92)	21.25 (10)	0.66 (161)	18.06 (23)
Spring	1849	0.32	12.67	0.43 (36)	12.26 (48)	0.45 (42)	12.16 (48)	0.49 (55)	11.59 (51)
Summer	2824	0.27	14.61	0.45 (66)	13.54 (42)	0.51 (89)	13.05 (45)	0.56 (109)	12.53 (47)
Autumn	1776	0.37	18.59	0.53 (42)	16.98 (28)	0.6 (61)	16.2 (31)	0.69 (84)	14.52 (38)

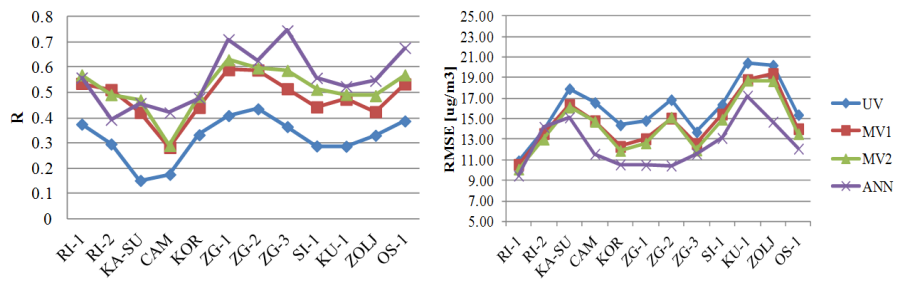

Figure 5. Comparison of linear correlation coefficient (R) (left) and Root Mean Square Error (RMSE) (right) for ground-based stations for four models: univariate linear regression model (UV), multivariate linear regression model with first-order effects (MV1), multivariate linear regression model with first and second-order effects (MV2) and Artificial neural network (ANN).

overestimation of PM10 values, and positive to underestimation of PM10 concentrations. The spread of residuals is highest and most spatially heterogeneous for winter and most homogenous for summer. For winter, PM10 concentrations are mostly underestimated for the majority of continental stations (SI-1, KU-1, ZG-1, ZG-2, ZG-3) and mostly overestimated for majority of coastal stations (RI-2, KA-SU, CAM, KOR). This implies that two separate ANN models for continental and for coastal Croatia might give better results. The problem with this would be definition of the border between those two parts on which the model could be applied. High positive residuals are related to episodes with high observed PM10 concentrations that ANN model underestimated and could not explain with independent variables. Generally, the model performs better for PM10 values lower than 40 μgm^{-3} (representing 84% of data) than for higher PM10 values (Figure 7). This could be due to very low number of samples with high PM10 values (only 1.5% of PM10 measurements are higher than 80 μgm^{-3}). Values lower than 20 μgm^{-3} are mostly overestimated and values higher than 20 μgm^{-3} are mostly underestimated where the discrepancies between observed and estimated PM10 values increase with increase of PM10 values (Figure 7). Differences in annual means between observed and estimated PM10 concentrations for 5 years and 12 stations show that 50% of annual means are within range from -2.9 to 2.3 μgm^{-3}; thus, PM10 estimation represents a relatively good proxy for annual mean of PM10 mass concentrations.

The uncertainties in estimated concentrations originate from variation in satellite retrieval uncertainties, uncertainties in measured PM10 data and modeled meteorological fields as well as from spatio-temporal averaging, as each of these uncertainties propagates to modeling results. Other factors that control PM10 concentrations, such as spatio-temporal variations of emissions and vertical gradients of meteorological variables have not been included in the analysis and might improve the estimations. The best results may be achieved using information on aerosol vertical profile from satellite or ground-based lidars, if available.

3.5. Examples of estimated PM10 spatial maps

Spatial maps of surface PM10 mass concentrations have been derived using ANN model that demonstrated the best overall performance, as discussed in the previous paragraphs. Seasonal and annual mean PM10 maps (Figures 8 and 9) have been estimated from gridded AOD values available in the period 2008-2012, and meteorological fields from WRF model on a daily basis and av-

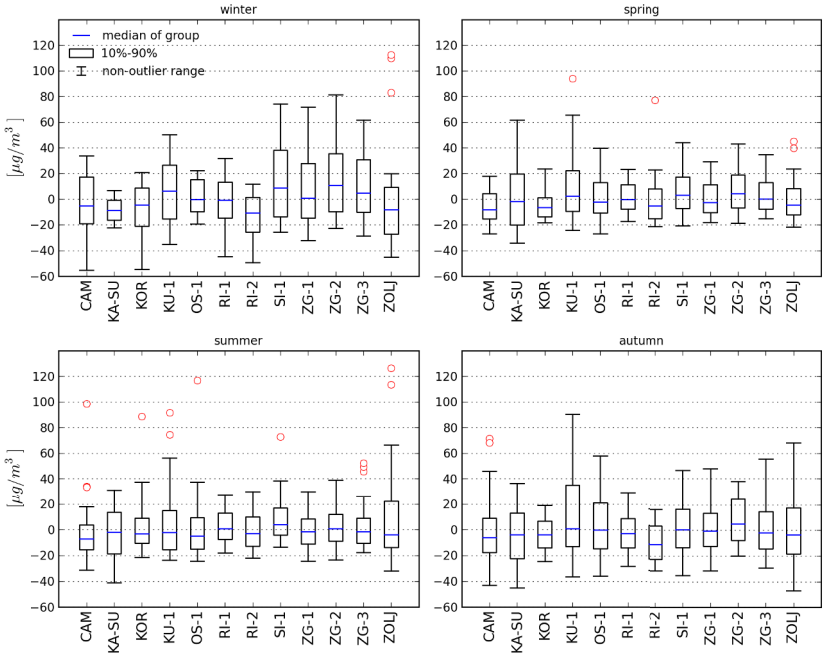

Figure 6. Statistics of PM10 residuals (observed – estimated values; Y - axis) by seasons (graph titles) and stations (X – axis). Outliers: values higher than $RES_{90\%}+1.5*(RES_{90\%}-RES_{10\%})$ and lower than $(RES_{10\%}-1.5*(RES_{90\%}-RES_{10\%})$, where RES is PM10 residual.

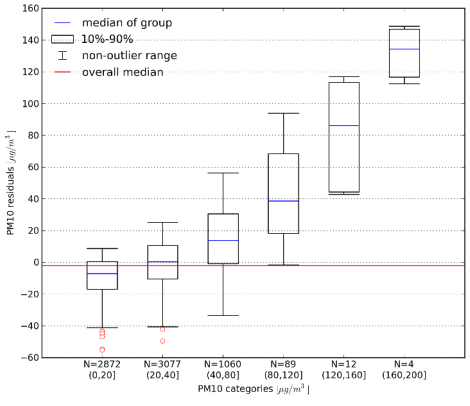

Figure 7. Statistics of ANN PM10 residuals (observed – estimated values; Y-axis) by PM10 categories (X-axis). Outliers: values higher than $RES_{90\%}+1.5*(RES_{90\%}-RES_{10\%})$ and lower than $(RES_{10\%}-1.5*(RES_{90\%}-RES_{10\%})$, where RES is PM10 residual.

eraged by seasons, after which seasonal maps were averaged to get map of annual means. The generated seasonal mean maps show reasonable spatio-temporal distribution of PM10 concentrations, with the highest values in the central, northern and eastern (agricultural) part of Croatia during winter and autumn, indicating areas at risk of exceeding limit values set by EU. High estimated PM10 values at coastal and in the southern part of Croatia at the land-sea boundary are probably a consequence of application of the land algorithm to fragments of sea, which is likely to lead to high AOD values [8]. In these areas (including islands), there are no known sources of pollution that could cause higher values than in the continental area. Uncertainty in AOD retrievals over coastal areas hinders PM10 estimates, and has to be further analyzed and validated using ground-based AOD measurements, which are currently not available.

The Croatian air quality network has very recently been upgraded to rural/background stations that provide better area coverage and also include PM2.5 measurements. When validated data from these stations becomes available, the model will be reassessed. These results will also be further combined and compared with the results of an atmospheric chemical transport model.

4. Summary and conclusions

This study shows promising potential for air quality monitoring and exposure assessment using satellite remote sensing and modeled meteorological fields, as extension to measurements of PM10 over Croatia at the locations where measurements do not exist. This approach can be applied to other countries with sparse PM10 monitoring

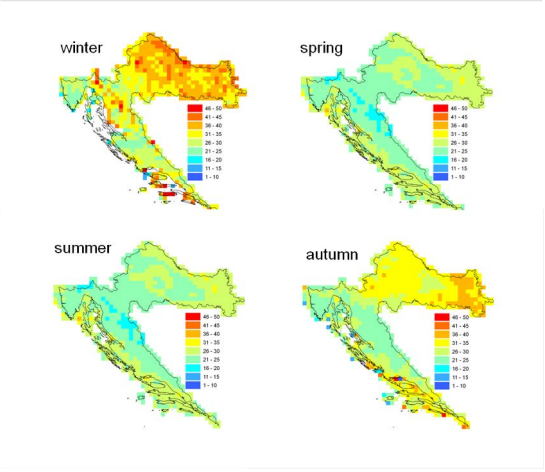

Figure 8. Estimated seasonal mean PM10 mass concentrations for period 2008-2012 using ANN model. PM10 is given in μgm^{-3}.

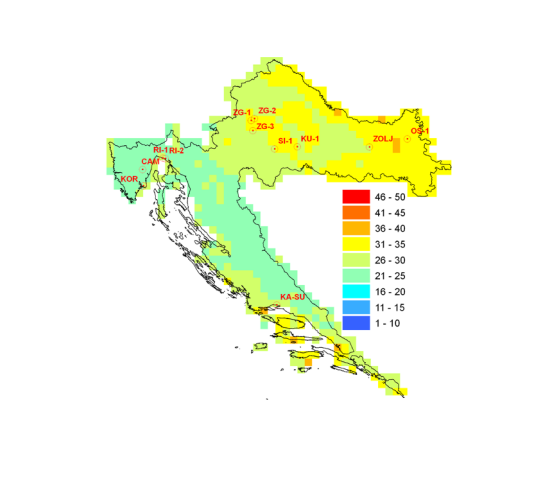

Figure 9. Estimated annual mean surface PM10 mass concentrations (given in μgm^{-3}) derived with ANN model. Labels represent locations of ground-based PM10 measurement stations.

stations and/or with lack of emission inventories needed for running atmospheric chemical transport models, since the satellite AOD data are globally available with high spatial and temporal resolution in near-real time, and the meteorological fields can be obtained from a meteorological model, for which initial and boundary conditions are globally and regularly available. The advantage of this approach is that it doesn't require extensive effort to derive emission inventories and the cost is much lower than the cost of maintaining a single measurement station. Moreover, derived spatial maps of PM10 can be used for the assessment, spatial optimization and refinement of existing ground-based monitoring networks, since they indicate areas of increased aerosol loading. Combined with trajectory models, AOD data and spatial (daily) PM10 maps can provide guidance to air quality modeling and forecasting community in determining possible aerosol movement or studying transboundary air pollution. Since the derived PM10 maps provide better spatial coverage than ground measuremens, it can also be usefull as additional information for chemical transport models calibration and validation.

In this study, the relationship between satellite derived AOD and PM10 was used to obtain surface PM10 mass concentrations. The PM10-AOD relationship was analyzed using a linear univariate model (UV) that estimates PM10 concentrations using only AOD as the input variable, and more complex multivariate models (MV1, MV2 and ANN) that estimate PM10 concentrations using 5 years (2008-2012) of meteorological fields from meteorological WRF model, as well as MODIS AOD and CF data. All the models demonstrated better performance when seasonality is included as predictor. Among models that include seasonality, UV model has demonstrated the poorest overall performance (R=0.32), suggesting that additional information is needed to convert columnar measurements to surface values.

The addition of meteorological variables in multivariate models significantly improved PM10 concentration estimation, where the most complex ANN model showed the highest percentage of increase in R (90.63%) relative to UV model, whereas the MV1 and MV2 models led to increase of R of 53.1% and 65.6%, respectively. The performance of the models varies with seasons and with geographical locations. The ANN model demonstrated the highest rate of improvement for all seasons compared to other models, with the highest percentage increase of R compared to UV model of 161% for winter. ANN model performs the best during autumn (R=0.69) and winter (R=0.66) with intermediate success during summer (R=0.56) and spring (R=0.49). The seasonal differences in the models' performance may be associated with seasonal variations in aerosol vertical profile that affect the AOD-PM10 relationship, seasonally variable transport of aerosol in upper layers, seasonal variations of uncertainties in AOD related to temporal heterogeneity of aerosol type and composition and seasonal variations in accuracy of meteorological parameters obtained by WRF model (caused by complex topography and climatic characteristics of the study area) that are subject to further research.

The average improvement rate of R over all stations is 50.3% for MV1, 61.3% for MV2 and 74.6% for ANN, compared to the UV model. Performance of all models is generally better for continental than for coastal stations, which may be explained with higher uncertainties in satel-

lite AOD retrievals due to mixed land and sea surfaces, as well as to higher uncertainties of modeled meteorological parameters at coastal area with complex topography.

Sensitivity analysis for ANN has shown that all tested independent variables (AOD, PBLH, WS, Un, Vn, T, P, CF) were significant predictors of PM10.

Despite to the fact that the estimation of PM10 concentrations from satellite AOD data and meteorological parameters provides a good proxy for seasonal and annual average values for the entire country, there is still unexplained variability in the PM10-AOD relationship, which remains a challenge for future work, especially related to estimation of episodic high PM10 values.

Further research with 1) use of more complex neural networks, 2) configurations of meteorological model including better vertical and horizontal model resolution and different schemes for boundary layer, 3) inclusion of vertical distribution of meteorological parameters and 4) generation of separate models for continental and coastal parts, may lead to better results. Finally, consideration of aerosol vertical profiles, from satellite or ground-based lidars, could improve our understanding of the PM10-AOD relationship and improve PM10 estimates in the future.

Due to lack of data from rural and background stations, the models were established with data mainly from urban stations, thus being more representative for urban areas than for rural areas. Background stations have recently been established and when data becomes available, the model will be revised to include those stations.

Additionally, the 3 km resolution MODIS AOD product expected as part of the Collection 6 and the newly developed Multi-Angle Implementation of Atmospheric Correction (MAIAC) algorithm [35] with 1 × 1 km spatial resolution may give better results, with possibility of recognizing spatial variability within larger urban areas.

Acknowledgments

This Study is part of Eureka E!5460 WEBAIR-2 project: "Web and 3G mobile phone based air quality management: particulates, public health, co-benefits". The project is co-financed by the Government of the Republic of Croatia (Ministry of Science, Education and Sports) under the program EUREKA. PM10 data were obtained from Croatian Environment Agency, Air Quality Database. MODIS data were obtained from the Level 1 and Atmosphere Archive and Distribution System (LAADS) at Goddard Space Flight Center (GSFC). The authors acknowledge assistance of Mr. Igor Tomažić with optimisation of satellite data aquisition procedure. The Cyprus consortium expresses their gratitude to the Cyprus Research Promotion Foundation for their funding of the project.

Appendix A: QUANTITATIVE DESCRIPTION OF MODELS

1. Description of univariate (UV) and multivariate linear regression models (MV1 and MV2) in Variant 1

The general form of multivariate linear regression models is given by

$$Y = \alpha_0 + \alpha_1(Var_1) + \ldots + \alpha_n(Var_n). \qquad \text{(A1)}$$

The dependent variable Y on the left side is the measured surface PM10 concentration. The independent continuous variables ($Var_1 \ldots Var_n$) are on the right side. The parameters $\alpha_{0\ldots}\alpha_n$ represent regression coefficients for independent variables.

The univariate linear model (UV) has only one (n = 1) independent continuous variable (AOD). The multivariate linear model with first order effects (MV1) has 9 (n = 9) independent continuous variables (AOD, PBLH, WS, RH, Un, Vn, T, P, CF). The multivariate linear model with first and second order effects (MV2) has first (linear) and second order (quadratic) terms of the same continuous variables as in MV1 model.

The described empirical models were optimized through use of Mallows' CP criterion [29], resulting in models with best subsets of independent continuous variables. The regression parameters of optimized models (UV, MV1 and MV2) are given in Table 4.

2. Description of univariate (UV) and multivariate linear regression models (MV1 and MV2) in Variant 2

In Variant 2, a categorical variable "season" has been added to the above presented UV, MV1, and MV2 models. The general form of these models is given by

$$\begin{aligned} Y =& \alpha_0 + \alpha_1(Var_1) + \ldots + \alpha_n(Var_n) + \alpha_w(winter) \\ &+ \alpha_{sp}(spring) + \alpha_{su}(summer) + \alpha_{au}(autumn). \end{aligned} \qquad \text{(A2)}$$

The season (as categorical variable) is coded with sigma-restricted parameterization [29]. The regression parameters (estimates) for the optimized models (best subsets of independent variables defined by Mallows Cp criterion) for UV, MV1 and MV2 in Variant 2 are given in Table 5.

Table 4. Estimated parameters of the optimized empirical models (UV, MV1, MV2) in Variant 1 represented by Eq. A1.

Variant 1	UV				MV1				MV2			
Independent variables	**par est**	**std err**	**t**	**p(t)**	**par est**	**std err**	**t**	**p(t)**	**par est**	**std err**	**t**	**p(t)**
Intercept	**20.884**	0.304	68.680	<10-4	**−150.242**	37.014	−4.06	<10-4	**61.367**	1.657	37.04	<10-4
AOD	**35.991**	1.454	24.760	<10-4	**42.476**	1.417	29.98	<10-4	**58.790**	2.401	24.48	<10-4
WS	–	–	–	–	**−1.485**	0.093	−15.96	<10-4	**−1.866**	0.089	−21.08	<10-4
PBLH	–	–	–	–	**−5.487**	0.438	12.54	<10-4	**−19.095**	1.108	−17.23	<10-4
RH	–	–	–	–	**−0.257**	0.022	−11.86	<10-4	**−0.282**	0.021	−13.48	<10-4
Vn	–	–	–	–	**3.388**	0.321	10.55	<10-4	**3.053**	0.318	9.60	<10-4
Un	–	–	–	–	**2.451**	0.286	8.57	<10-4	–	–	–	–
CF	–	–	–	–	**−9.848**	1.522	−6.47	<10-4	–	–	–	–
P	–	–	–	–	**0.191**	0.036	5.33	<10-4	–	–	–	–
T	–	–	–	–	–	–	–	–	**−1.205**	0.103	<10-4	11.70
PBLH^2	–	–	–	–	–	–	–	–	**4.673**	0.389	<10-4	12.02
T^2	–	–	–	–	–	–	–	–	**0.032**	0.003	<10-4	11.96
AOD^2	–	–	–	–	–	–	–	–	**−34.796**	3.310	<10-4	10.51

par est - parameter estimate; std err - standard error of the parameter estimate; t - t-statistics. p(t) - probability of t-statistics (that parameter estimated is equal to zero, i.e. without significant contribution to the model estimation).

Table 5. Estimated parameters of the optimized empirical models (UV, MV1, MV2) in Variant 2 represented by Eq. A2.

Variant 2	UV				MV1				MV2			
Independent variables	**par est**	**std err**	**t**	**p(t)**	**par est**	**std err**	**t**	**p(t)**	**par est**	**std err**	**t**	**p(t)**
Intercept	**21.486**	0.314	68.45	<10-4	**−119.994**	38.066	−3.16	0.0016	**47.437**	1.497	31.70	<10-4
Winter	**4.404**	0.502	8.77	<10-4	**9.105**	0.616	14.79	<10-4	**6.651**	0.632	10.52	<10-4
Spring	**−3.822**	0.353	−10.84	<10-4	**−3.880**	0.343	−11.30	<10-4	**−2.254**	0.379	−5.95	<10-4
Summer	**−2.395**	0.310	−7.74	<10-4	**−6.427**	0.460	−13.98	<10-4	**−7.264**	0.452	16.080	<10-4
Autumn	**0.000**	–	–	–	**0.000**	–	–	–	**0.000**	–	–	–
AOD	**38.968**	1.459	26.71	<10-4	**42.789**	1.418	30.18	<10-4	**57.920**	2.409	24.04	<10-4
WS	–	–	–	–	**−1.566**	0.093	−16.79	<10-4	**−1.936**	0.086	−22.44	<10-4
PBLH	–	–	–	–	**−3.977**	0.457	−8.70	<10-4	**−19.461**	1.106	−17.60	<10-4
RH	–	–	–	–	**−0.229**	0.022	−10.60	<10-4	**−0.002**	0.000	−11.33	<10-4
Vn	–	–	–	–	**3.617**	0.328	11.01	<10-4	**3.228**	0.314	10.27	<10-4
Un	–	–	–	–	**2.315**	0.282	8.22	<10-4	–	–	–	–
CF	–	–	–	–	**−9.931**	1.498	−6.63	<10-4	–	–	–	–
P	–	–	–	–	**0.153**	0.037	4.17	<10-4	–	–	–	–
T	–	–	–	–	**0.355**	0.044	8.12	<10-4	**−0.971**	0.121	−8.06	<10-4
PBLH^2	–	–	–	–	–	–	–	–	**5.459**	0.385	14.20	<10-4
T^2	–	–	–	–	–	–	–	–	**0.037**	0.003	11.51	<10-4
AOD^2	–	–	–	–	–	–	–	–	**−35.531**	3.248	−10.94	<10-4

par est - parameter estimate; std err - standard error of the parameter estimate; t - t-statistics. p(t) - probability of t-statistics (that parameter estimated is equal to zero, i.e. without significant contribution to the model estimation).

References

[1] European Environment Agency. The European environment — state and outlook. Luxembourg: Publications Office of the European Union, 2010, ISBN 978-92-9213-152-4, doi:10.2800/57792 (2010)

[2] Croatian Environment Agency. Annual report of air quality monitoring in Croatia for 2011. Document number: 25-12-2212/55 (2011) (www.azo.hr)

[3] Villeneuve P.J., Goldberg M.S., Krewski D., Burnett R.T., Chen Y., Fine particulate air pollution and all-cause mortality within the Harward six-cities study:variations in risk by period of exposure. *Annals of Epidemiology*, 2002, 12, 568-576

[4] Tian J., Chen D., Spectral, spatial, and temporal sensitivity of correlating MODIS aerosol optical depth with ground-based fine particulate matter (PM2.5) across southern Ontario. *Can. J. Remote Sensing*, 2010, 36, 119-128

[5] Koelemeijer R.B.A., Homan C.D., Matthijsen, J., Comparison of spatial and temporal variations of aerosol optical thickness and particulate matter over Europe. *Atmospheric Environment*, 2006, 40, 5304-5315

[6] Al-Saadi J., Szykman J., Pierce R. B., Kittaka C., Neil D., Chu D. A., Remer L., Gumley L., Prins E., Weinstock L., MacDonald C., Wayland R., Dimmick F. and Fishman J., Improving national air quality forecasts with satellite aerosol observations. *Bulletin of the American Meteorological Society*, 2005, 86, 1249–1261, doi:10.1175/BAMS-86-9-1249

[7] Engel-Cox J.A., Holloman C.H., Coutant B.W., Hoff R.M., Qualitative and quantitative evaluation of MODIS satellite sensor data for regional and urban scale air quality. *Atmos. Environ.*, 2004, 38, 2495–2509

[8] Chu D.A., Kaufman Y.J., Zibordi G., Chern J.D., Mao J., Li C., Holben B.N., Global monitoring of air pollution over land from the Earth Observing System-Terra Moderate Resolution Imaging Spectrora-diometer (MODIS), *J. Geophys. Res.*, 2003, 108(D21), 4661, doi:10.1029/2002JD003179

[9] Wang J., Christopher S.A., Intercomparison between satellite-derived aerosol optical thickness and PM2.5 mass: implications for air quality studies. *Geophysical Research Letters*, 2003, 30, 2095

[10] Gupta P., Christopher S.A., Wang J., Gehrig R., Lee Y.C., Kumar N., Satellite remote sensing of particulate matter and air quality over global cities. *Atmos. Environ.*, 2006, 40, 5880–5892

[11] Dinoi A., Perrone M.R., Burlizz P., Application of MODIS Products for Air quality studies Over Southeastern Italy. *Remote Sens.*, 2010, 2, 1767-1796

[12] Gupta P., Christopher S.A., Particulate matter air quality assessment using integrated surface, satellite, and meteorological products: 1. Multiple regression approach. *J. Geophys. Res.*, 2009, 114, D14205, doi:10.1029/2008JD011496

[13] Engel-Cox J A., Hoff R.M., Rogers R., Dimmick F., Rush A.C., Szykman J.J., Al-Saadi J., Chu D.A., Zell E.R., Integrating lidar and satellite optical depth with ambient monitoring for 3-dimensional particulate characterization. *Atmos. Environ.*, 2006, 40, 8056–8067

[14] Li C., Hsu N.C., Tsay S.C., A study of the potential application of satellite data in air quality monitoring and forecasting. *Atmos. Environ.*, 2011, 35, 3663-3675

[15] Gupta P., Christopher S.A., Particulate matter air quality assessment using integrated surface, satellite, and meteorological products: 2. A neural network approach. *J. Geophys. Res.*, 2009, 114, D20205, doi:10.1029/2008JD011497

[16] Wu Y., Guo J.Z.X., Tian X., Zhang J., Wang Y., Duan J., Li X., Synergy of satellite and ground based observations in estimation of particulate matter in eastern China. *Science of the Total Environment*, 2012, 433, 20-30

[17] Levy R.C., Remer L., Tanre D., Matoo S., Kaufman, Y.J., Algorithm for remote sensing of tropospheric aerosol over dark targets from MODIS: collections 005 and 051:Revision 2, 2009. http://modis-atmos.gsfc.nasa.gov/_docs/ATBD_MOD04_C005_rev2.pdf.

[18] Remer L.A., Kaufman Y. J., Tanré D., Mattoo S., Chu D. A., Martins J. V, Li R.-R., Ichoku C., Levy R.C., Kleidman R.G., Eck T.F., Vermote E. and Holben B.N., The MODIS aerosol algorithm, products, and validation. *J. Atmos. Sci.*, 2005, 62, 947–973, doi:10.1175/JAS3385.1

[19] Chu D.A., Kaufman Y.J., Ichoku C., Remer L.A., TanreD., Holben B.N., Validation of MODIS aerosol optical depth retrieval over land. *Geophysical research letter*, 2002, 29, 10.1029/2001GL013205

[20] Skamarock W.C., Klemp J.B., Dudhia J., Gill D.O., Barker D.M., Wang W., Powers J.G., A description of the Advanced Research WRF Version 2, NCAR/TN-468+STR, NCAR TECHNICAL NOTE, 88., 2007

[21] Chen F., Janjic Z., K. Mitchell. Impact of atmospheric surface layer parameterization in the new land-surface scheme of the NCEP Mesoscale Eta numerical model. *Bound.-Layer Meteor.*, 1997, 185, 391-421

[22] Chen F., Dudhia J., Coupling an Advanced Land

Surface-Hydrology Model with the Penn State-NCAR MM5 Modeling System. Part I: Model Implementation and Sensitivity. *Mon. Wea. Rev.*, 12001, 29, 569-585

[23] Hong S.Y., Jade J.O., The WRF Single Moment 6 Class Microphysics Sheme (WSM6). *Journal of the Korean Meteorological Society*, 42, 2, 2006, 129-151

[24] Mlawer E.J., Taubman S.J., Brown P.D., Iacono M.J., Clough S.A., Radiative transfer for inhomogeneous atmosphere: RRTM, a validated correlated-k model for the long-wave, *J. Geophys. Res.*, 102(D14), 1997, 16663–16682

[25] Hong S.Y., Dudhia J., Chen S.H., A Revised Approach to Ice Microphysical Processes for the Bulk Parameterization of Clouds and Precipitation, *Mon. Wea. Rev.*, 2004, 132, 103–120

[26] Kain J.S., Fritsch J.M., Convective parameterization for mesoscale models: The Kain- Fritsch scheme. The representation of cumulus convection in numerical models. *Meteor. Monogr.*, 1993, 24, 165-170

[27] Hrust L., Klaić B., Križan Z., Antonić J., Hercog O., Neural network forecasting of air pollutants hourly concentrations using optimized temporal averages of meteorological variables and pollutant concentrations. *Atm. Environ.*, 2009, 43, 5588-5596

[28] Gardner M.V., Dorling S.R., Neural network modeling and prediction of hourly Nox nad NO_2 concentration in urban air in London. *Atmos. Environ.* 1999, 33, 709-719

[29] Mallows C.L., Some Comments on CP", *Technometrics*, 1973, 15 (4), 661-675

[30] Stevens J., Applied Multivariate Statistics for the Social Sciences. Taylor & Francis, New York, 2002

[31] Bishop C.M., Neural networks for Pattern Recognition. Cylerdon Press, Oxford, 1995

[32]] Haykin S., Neural network: a Comprehensive Foundation. Prentice Hall, Upper Saddle River, NJ, 1999

[33] Wojciechowski M., Feed-forward neural network for python, Technical University of Lodz (Poland), Department of Civil Engineering, Architecture and Environmental Engineering, http://ffnet.sourceforge.net/, ffnet-0.7, 2011

[34] Riedmiller M., Braun H., A Direct Adaptive Method for Faster Backpropagation Learning: The RPROP Algorithm, in H.Ruspini, editor, *Proceedings of the 1993 IEEE International Conference on Neural Networks (ICNN)*, San Francisco, USA, 1993, 586-591, doi: 10.1109/ICNN.1993.298623

[35] Lyapustin A.,Wang Y., Laszlo I., Kahn R., Korkin S., Remer L., Levy R., Reid J.S., Multiangle implementation of atmospheric correction (MAIAC): 2. Aerosol algorithm. *J. Geophys. Res.*, 2011, 116, D03211